

Published in final edited form as:

*Dev Biol.* 2013 August 1; 380(1): . doi:10.1016/j.ydbio.2013.04.033.

## Zebrafish *Zic2a* and *Zic2b* regulate neural crest and craniofacial development

Jessica J. TeSlaa<sup>1,2</sup>, Abigail N. Keller<sup>1</sup>, Molly K. Nyholm<sup>1,3</sup>, and Yevgenya Grinblat<sup>1,2,\*</sup>

<sup>1</sup>Departments of Zoology and Neuroscience, University of Wisconsin, Madison, WI, 53706, USA

<sup>2</sup>Cellular and Molecular Biology Training Program, University of Wisconsin, Madison, WI, 53706, USA

### Abstract

Holoprosencephaly (HPE), the most common malformation of the human forebrain, is associated with defects of the craniofacial skeleton. *ZIC2*, a zinc-finger transcription factor, is strongly linked to HPE and to a characteristic set of dysmorphic facial features in humans. We have previously identified important functions for zebrafish *Zic2* in the developing forebrain. Here, we demonstrate that *ZIC2* orthologs *zic2a* and *zic2b* also regulate the forming zebrafish craniofacial skeleton, including the jaw and neurocranial cartilages, and use the zebrafish to study *Zic2*-regulated processes that may contribute to the complex etiology of HPE. Using temporally controlled *Zic2a* overexpression, we show that the developing craniofacial cartilages are sensitive to *Zic2* elevation prior to 24hpf. This window of sensitivity overlaps the critical expansion and migration of the neural crest (NC) cells, which migrate from the developing neural tube to populate vertebrate craniofacial structures. We demonstrate that *zic2b* influences the induction of NC at the neural plate border, while both *zic2a* and *zic2b* regulate NC migratory onset and strongly contribute to chromatophore development. Both *Zic2* depletion and early ectopic *Zic2* expression cause moderate, incompletely penetrant mispatterning of the NC-derived jaw precursors at 24hpf, yet by 2dpf these changes in *Zic2* expression result in profoundly mispatterned chondrogenic condensations. We attribute this discrepancy to an additional role for *Zic2a* and *Zic2b* in patterning the forebrain primordium, an important signaling source during craniofacial development. This hypothesis is supported by evidence that transplanted *Zic2*-deficient cells can contribute to craniofacial cartilages in a wild-type background. Collectively, these data suggest that zebrafish *Zic2* plays a dual role during craniofacial development, contributing to two disparate aspects of craniofacial morphogenesis: (1) Neural crest induction and migration, and (2) early patterning of tissues adjacent to craniofacial chondrogenic condensations.

### Keywords

zebrafish; *Zic*; craniofacial cartilage; forebrain; holoprosencephaly

---

© 2013 Elsevier Inc. All rights reserved.

\*Correspondence: ygrinblat@wisc.edu.

<sup>3</sup>Current address: CELLSSCRIPT, Inc., 726 Post Road, Madison, WI 53713

**Publisher's Disclaimer:** This is a PDF file of an unedited manuscript that has been accepted for publication. As a service to our customers we are providing this early version of the manuscript. The manuscript will undergo copyediting, typesetting, and review of the resulting proof before it is published in its final citable form. Please note that during the production process errors may be discovered which could affect the content, and all legal disclaimers that apply to the journal pertain.

## Introduction

The complex patterning and morphogenesis of the craniofacial skeleton gives rise to the wide morphological variation in facial structure among vertebrates. Disruptions in normal craniofacial development result in defects ranging from mild dysmorphologies to more severe outcomes, including cleft palate and cyclopia (Wilkie and Morris-Kay, 2001). In humans, dysmorphic facial features and craniofacial defects are often associated with malformations of the brain such as Dandy-Walker malformation (DWM) and HPE (Dubourg et al., 2007; Mademont-Soler et al., 2010). The extent of interdependence between brain and craniofacial morphology, the subject of recent studies, is not fully understood (Le Douarin et al., 2012; Marcucio et al., 2011).

Vertebrate craniofacial development depends heavily on the contribution of chondrogenic precursors from the cephalic NC (Cordero et al., 2010; Minoux and Rijli, 2010). The NC is induced at the border of the neural ectoderm during gastrulation and subsequently exits the neural epithelium and migrates throughout the developing embryo (Milet and Monsoro-Burq, 2012). NC cells from the posterior diencephalon and midbrain contribute to the anterior neurocranial cartilages (Wada et al., 2005), while NC cells from the hindbrain populate the first two pharyngeal arches (PAs) and form the jaw cartilages (Lumsden et al., 1991; Schilling and Kimmel, 1994; Schilling and Kimmel, 1997). Development of the facial complex is disrupted by mutations in genes that regulate NC development and survival, e.g. *arl6ip1* (Tu et al., 2012), *dlx2a* (Sperber et al., 2008), *Myo10* (Nie et al., 2009) *sox9b* (Yan et al., 2005) and *tfap2* genes (Barrallo-Gimeno et al., 2004; Knight et al., 2003; Li and Cornell, 2007).

Establishment of the craniofacial cartilages also relies on appropriate patterning and morphogenesis of surrounding tissues (Szabo-Rogers et al., 2010). Developing craniofacial cartilages receive important patterning cues from neural epithelium (Marcucio et al. 2005; Chong et al., 2012), pharyngeal endoderm (Couly et al., 2002; Haworth et al., 2007; Ruhin et al., 2003), facial ectoderm, (Hu and Marcucio, 2009; Reid et al., 2011) and olfactory placodes (Szabo-Rogers et al., 2009). The NC cells themselves constitute an important piece of this signaling network (Bonilla-Claudio et al., 2012; Jeong et al., 2004). The forebrain, facial ectoderm and pharyngeal endoderm are each a source of Hh signaling, a particularly important patterning cue during craniofacial development. Hh signaling promotes proliferation and differentiation of chondrogenic precursors, and global disruption of Hh signaling causes severe defects in jaw and neurocranial cartilages (Ahlgren and Bronner-Fraser, 1999; Schwend and Ahlgren, 2009; Swartz et al., 2012). In zebrafish, Hh signaling from the ventral forebrain primordium plays a key role in the development of the anterior neurocranium (Wada et al., 2005) and stomodeal ectoderm, which serves as a substrate for chondrogenic NC condensation (Eberhart et al., 2006).

Zic genes encode a family of zinc finger transcription factors with documented roles in NC development and forebrain morphogenesis and patterning (Merzdorf, 2007; Maurus and Harris, 2009). *ZIC2* mutations in humans are linked to HPE and a characteristic craniofacial morphology (Brown et al., 1998; Mercier et al., 2011; Solomon et al., 2010a). Mice homozygous for hypomorphic or null alleles of *Zic2* develop with HPE-like forebrain defects and hypoplastic NC derivatives (Elms et al., 2003; Nagai et al., 2000; Warr et al., 2008). Homozygous mouse mutants in *Zic5*, a gene closely linked to and co-expressed with *Zic2*, exhibit a shortened mandible, which is fused at the midline (Inoue et al., 2004). *Zic2* (Brewster et al., 1998; Nakata et al., 1998) and *Zic5* (Nakata et al., 2000) overexpression induces NC genes in *Xenopus*. Whether the craniofacial dysmorphology in mammalian Zic mutants is solely the outcome of Zic regulation of NC generation is unknown.

The zebrafish genome encodes two orthologs of mammalian *ZIC2*, *zic2a* and *zic2b* (Toyama et al., 2004). Our previous work demonstrated a role for *zic2a* during forebrain development (Sanek et al., 2008; Sanek et al., 2009). We showed that *Zic2a* interacts with the Hh signaling pathway to pattern the diencephalon and optic stalk/retinal interface. In this study, we investigate the roles of the zebrafish *ZIC2* orthologs in craniofacial development. Based on the previously documented role of *zic* genes in NC development and their association with craniofacial dysmorphologies, we hypothesized that *Zics* regulate early NC lineages that subsequently give rise to craniofacial structures. We find evidence for zebrafish *zic2a* and *zic2b* involvement in early NC induction and migratory onset and demonstrate a requirement for *zic2a* and *zic2b* regulation of the pigment cell lineage. However, *zic* contribution to chondrogenic NC formation may not be the sole cause of the profound craniofacial defects observed in *Zic2*-depleted and overexpressing embryos. Our data suggest a second, non-cell autonomous role for *Zic2a* and *Zic2b* in patterning tissues adjacent to craniofacial cartilages, e.g. the ventral forebrain primordium, which in turn promote post-migratory development of NC-derived chondrogenic precursors.

## Material and methods

### Zebrafish strains and embryo culture

Adult zebrafish were maintained according to established methods (Westerfield, 2000). Embryos were obtained from natural matings and staged according to Kimmel (Kimmel et al., 1995). The *11XUAS:zic2aYFP* transgene was constructed in the pBH-UAS-mcs-YFP vector backbone, which contains Tol2 sites and a *cmc2:Cherry* cassette for independent verification of transgene presence (vector provided by M. Nonet; sequence information at <http://thalamus.wustl.edu/nonetlab/ResourcesF/Zebrafish.html>).

Tg(*11XUAS:zic2aYFP;cmc2:Cherry*) stable transgenics were produced using established methods (Kawakami et al., 2004). The Tg(*hsp70l:Gal4VP16*) line was provided by B. Appel, Vanderbilt University (Inbal et al., 2007; Takada and Appel, 2011)

### Knockdown assays

Gene-specific antisense oligonucleotide morpholinos (MO) and standard control MO were purchased from GeneTools (Philomath, OR). The *zic2a* splice-blocking MO (*zic2aMO*) and *zic2a* translation-blocking MOs (*zic2aAUGMO* and *zic2aproxMO*), have been described (Nyholm et al., 2007). *Zic2b* morpholinos were designed against the translational start site (*zic2b* AUG MO: TATTGACCAAAGAATGCGTAAAGAC) and the exon 1–intron 2 splice donor site (*zic2b* MO: ATTGAAATAATTACCAGTGTGTGTC) of *zic2b*. MOs were diluted in 1X Danieau buffer (Nasevicius and Ekker, 2000) to 1–2ng/nl (*zic2aMO*), 6–8ng/nl (*zic2aAUG+zic2aproxMO*, injected together; henceforth referred to as *zic2aAUGMO*), 2–4ng/nl (*zic2bMO*), 4–8ng/nl (*zic2b* AUG MO) or 3–4ng/nl (*conMO*). Injections were carried out at the 1–2 cell stage on a Picospritzer III (Parker Instrumentation) or a PLI100 (Harvard Apparatus). Each injected embryo received 0.5–1nl of either *zic2aMO* or *zic2bMO*. Double *zic2* morphants were injected twice, with 0.5nl of each MO. To test the efficacy of the *zic2bMO*, RNA was extracted from embryos injected with *zic2bMO* and used to generate cDNA using the iScript kit (BioRad). PCR was performed using primers complimentary to sequences in exon 1 (5'-TGGGCGCGTTCAAAGT-3') and exon 3 (5'-ATTGTGCCCCGCTGCTGTT-3'). Images show embryos injected with the *zic2a* or *zic2b* splice blocking MOs unless noted otherwise.

### Overexpression and rescue assays

*Zic2aYFP* overexpression was achieved by mating the Tg(*hsp70l:Gal4VP16*) line with the Tg(*11XUAS:zic2aYFP*) line. Upon heat shock induction, the resulting double transgenic embryos express *Zic2aYFP* fusion protein. Heat shocks were administered for one hour in a

37°C water bath. Heat-shocked embryos were allowed to recover at room temperature (25°C) or 29°C for approximately five hours and then sorted for YFP fluorescence. Heat-shocked YFP-negative siblings were used as controls. For rescue experiments using *zic2a*AUGMO, each clutch obtained from *Tg(hsp70l:Gal4VP16) x Tg(11XUAS:zic2aYFP)* pair mating was divided into three sibling groups: (1) uninjected, (2) conMO injected and (3) *zic2a*AUGMO injected. All embryos were subsequently heat shocked at 10hpf, and sorted for YFP fluorescence 10–12 hours post-heatshock. Note that YFP fluorescence was not observed in any of the *Zic2a*AUGMO-injected embryos, consistent with efficient MO-mediated knockdown of *Zic2a*YFP expression.

### In situ hybridization (ISH), histology and Alcian Blue staining

Antisense digoxigenin or fluorescein labeled RNA probes were transcribed using the MAXIScript kit (Ambion) from the following plasmid templates: *apob* (Thisse et al., 2001), *col2a1a* (Yan et al., 1995), *dlx2a* (Akimenko et al., 1994), *dlx3b* (Akimenko et al., 1994), *foxd3* (Odenthal and Nusslein-Volhard, 1998), *gch2* (Parichy et al., 2000), *mitfa* (Lister et al., 1999), *nkx2.2a* (Karlstrom et al., 2003), *pax2a* (Hoyle et al., 2004), *pitx2a* (Essner et al., 2000), *ptch2* (Vanderlaan et al., 2005), *snai1b* (Thisse et al., 1995), *sox9a* (Cresko et al., 2003), *sox10* (Dutton et al., 2001), *zic2a* (Grinblat and Sive, 2001) and *zic2b* (a kind gift from Becky Burdine and Alex Schier). Some embryos fixed at 2 and 3dpf were raised in 0.003% phenylthiohydroxyurea (PTU) to prevent pigment formation. ISH was carried out as previously described (Gillhouse et al., 2004). Differential interference contrast (DIC) images were obtained using an Axioskop2 Plus microscope with AxioVision software (Zeiss) or a Leica MZ FLIII with LAS v4.0 software. Stained embryos were embedded in Eponate 12 medium (Ted Pella) and 5–7µm sections were cut with a steel blade on an American Optical Company microtome. Nuclei were counterstained with Neutral Red. For Alcian Blue staining, zebrafish larvae were fixed in 4% paraformaldehyde overnight and stained according to Kimmel et al., 1998. Cartilages were dissected using sharpened tungsten needles and the preparations were flat-mounted in glycerol for imaging.

### Transplant assays

Embryos were injected at the 1-cell stage with either conMO or *zic2a*MO, and transplant donors were injected into the yolk with a mixture of 2% alexa568-dextran/3% biotin-dextran in 0.2M KCl (10,000 MW, lysine fixable, Molecular Probes). Embryos were dechorionated in 0.5X MBS on agarose pads. Cells were removed from the animal pole of sphere-stage donor embryos using finely ground glass capillary tubes with an outer diameter of 100–150µm, and injected into the animal pole of sphere-stage host embryos. The position of labeled donor tissue was examined at 24hpf on a fluorescent microscope. Confocal imaging was carried out on an Olympus FV1000 microscope with FV10-ASW software. Biotin was detected by incubation with an avidin-biotin-HRP complex (VectorLabs) and colorimetric reactions were developed with DAB.

### Quantitative real-time PCR

RNA was isolated from embryos using Trizol (Life Technologies) and cDNA was generated with the High Capacity cDNA archive kit from 1µg of input RNA (Applied Biosystems). Each 20µl reaction contained a final concentration of 0.2µM primers, 1X Power SYBR Green dye and 2µl of a 1:20 dilution of template cDNA. Primers designed to amplify a region spanning the exon 2 – exon 3 boundary of *sox10* (IDT) were generated using the PrimerExpress software (Applied Biosystems) and tested for efficiency as in Sanek et al., 2009. qPCR was performed on an Applied Biosystems StepOne Plus machine using the  $\Delta\Delta C_t$  method. Each of two biological replicates was loaded with three technical replicates on a single plate. *sox10* primer sequences were 5'-GGCTGCAGGGTCACCATT-3' and 5'-

AGGGCTGTGACTCTGACCTGTAG-3', and *ef1a* (used as the reference gene) primer sequences were 5'-CTTCTCAGGCTGACTGTGC-3' and 5'-CCGCTAGCATTACCCTCC-3'.

## Results

### Zebrafish *Zic2* regulates craniofacial development

In humans, mutations in *ZIC2* are associated with HPE and a mild but characteristic set of craniofacial dysmorphologies (Solomon et al., 2010a). Since zebrafish with reduced *Zic2a* levels display HPE-like forebrain defects (Sanek et al., 2008; Sanek et al., 2009), we asked whether zebrafish *ZIC2* orthologs, *zic2a* and *zic2b*, play roles in craniofacial development. To assess the role of *zic2a*, we injected a previously described *zic2a*-specific antisense morpholino oligonucleotide (*zic2a*MO) to knock down zebrafish *Zic2a* (Nyholm et al., 2007) and evaluated the effect on craniofacial cartilages with alcian blue staining at 5dpf (Fig. 1A–F). *Zic2a* depletion caused hypoplasia of the jaw in 72% of morphants (Fig. 1B). Defects ranged from the relatively mild improperly positioned hyoid arch (Fig. 1B', outlined) to more severely shortened jaw arches, (Fig. 1E). The most strongly affected *zic2a* morphants exhibited nearly complete deletion of the anterior pharyngeal and neurocranial cartilages (not shown, 20% of morphants).

To investigate a role for *zic2b* during craniofacial development, we designed a *zic2b*-specific splice-blocking morpholino (*zic2b*MO). Embryos injected with *zic2b*MO expressed reduced levels of full-length *zic2b* transcript and developed with neurulation defects comparable to *zic2a* morphants (Supplemental Fig. 1, Nyholm et al, 2009). *Zic2b* morphants showed mild craniofacial defects, with 35% displaying slight hypoplasia of the pharyngeal cartilages, while the remainder developed normally (Fig 1C,F). Similar results were obtained using a translation-blocking *zic2b*MO (data not shown). Together, these results suggest *zic2a* is required for normal craniofacial development, while *zic2b* plays a less critical role in this process (Fig. 1G).

To better understand when *Zic2a* exerts its effect on craniofacial development, we generated a transgenic line of fish, *Tg(11XUAS:zic2aYFP)*, that allowed temporally controlled overexpression of *Zic2a*YFP when crossed with the heat-inducible *Tg(hsp70l:Gal4VP16)* line. *Tg(hsp70l:Gal4VP16);Tg(11XUAS:zic2aYFP)* embryos expressed ubiquitous *Zic2a*YFP upon heat shock (HS) induction. After HS at 10hpf, *Zic2a*YFP-positive embryos developed with a distinct phenotype compared to their YFP-negative siblings. This phenotype included a shortened anterior-posterior axis, retinal coloboma and neurulation defects consistent with previously published roles of zebrafish *zic2a* in retinal and midbrain morphogenesis (Supplemental Fig. 2; Sanek et al., 2009; Nyholm et al, 2009). In addition, pharyngeal cartilages, which make up the basis of the forming jaw, were strongly affected, with shortening or inversion of the hyoid arch, and reduction of the ceratobranchial cartilages (Fig. 2A,E). HS induction at 14hpf was similarly disruptive, resulting in severely hypoplastic pharyngeal cartilages (Fig. 2B,F). However, when *Zic2a*YFP was induced at 17hpf, the effects were limited to mild shortening of the mandibular and hyoid elements in 50% of embryos (Fig. 2C,G). HS induction at 24hpf had no effect on the pharyngeal cartilages (Fig. 2D,H), suggesting that correct *Zic2a* expression prior to 24hpf is critical for pharyngeal cartilage development.

In addition to its effects on pharyngeal cartilages, *Zic2a*YFP induction at 10hpf caused abnormal proximity of the neurocranial trabecular cartilages to one another (Fig. 2I,J, asterisk in 2J). This defect was more pronounced after HS induction at 14hpf, with trabeculae fused at the midline (32% of embryos, asterisk in Fig. 2L), shortened (21%), or ablated completely (26%, Fig. 2K,L). The medial ethmoid plate was absent in 53% of *Zic2a*

overexpressors (arrow in Fig. 2L). These data show that both pharyngeal and neurocranial cartilages are profoundly affected by Zic2aYFP misexpression before 24hpf, and further support an important role for Zic2a in craniofacial development (Fig. 2M,N).

In order to confirm specificity of the craniofacial defects seen in *zic2* morphants and Zic2aYFP-expressing embryos, we used nonoverlapping translation-blocking morpholinos, *zic2aAUGMO*, to reduce Zic2a levels. Zic2aAUGMO-injected embryos developed with a range of pharyngeal cartilage defects comparable to those observed in Zic2aMO-injected morphants, but with a lower penetrance of these defects (58%, Supplemental Fig. 3). Notably, *zic2aAUGMO* effectively reduced Zic2aYFP levels and rescued the Zic2aYFP overexpression phenotype in *Tg(hsp70l:Gal4VP16) x Tg(11XUAS:zic2aYFP)* embryos (Supplemental Fig. 4).

To test whether chondrogenesis is disrupted prior to 5dpf in embryos with altered levels of Zic2a, we assayed expression of two chondrogenic markers, *sox9a* and *col2a1a*. *Sox9a*, which is required for chondrogenesis and marks the neurocranium and pharyngeal arches at 2dpf, was reduced in the anterior pharyngeal arches of *zic2a* morphants, and not expressed posterior to PA1 and PA2 (Fig. 3A,B). *Sox9a* is also expressed in the trabecular condensations, which failed to fully elongate in *zic2a* morphants (Fig. 3C,D). The medial ethmoid plate, visible by 2dpf in control embryos, failed to form in *zic2a* morphants (arrow in Fig. 3C). *Col2a1a*, the major collagen of cartilage expressed in the neurocranium, reiterated the shortened trabeculae and absence of the medial ethmoid plate in *zic2a* morphants (Fig. 3E,F). Similarly, following heat shock at 10hpf, Zic2aYFP-expressing embryos did not appropriately establish the bilateral chondrogenic condensations that prefigure the trabeculae (Fig. 3G,H). Collectively, results from knockdown and overexpression studies demonstrate a role for Zic2a in regulating early development of both pharyngeal and neurocranial cartilages, and show that Zic2a functions before 24hpf to correctly pattern craniofacial chondrogenic primordia.

### ***zic2a* and *zic2b* promote cranial neural crest induction and exit from the neural tube**

Many of the craniofacial structures that develop abnormally in embryos with altered levels of Zic2 are derived from NC cells. Based on the timing of Zic2 function, we hypothesized that the craniofacial defects in embryos with elevated or depleted Zic2a levels are due to a disruption in NC development. The expression patterns of *zic2a* and *zic2b* are consistent with an early role in NC induction. Both genes are expressed in the anterior neural plate, including the presumptive cranial NC, beginning at mid-gastrulation (Fig. 4A,B; Grinblat and Sive, 2001; Toyama et al., 2004). *Zic2a* shares a tight border with the non-neural ectodermal marker *dlx3b* through the end of gastrulation (Fig. 4C,D). As somitogenesis begins, *zic2a* levels are reduced in early NC, marked by expression of *foxd3* (Fig. 4E–H), and remain low through at least 5S (data not shown). In contrast, *zic2b* is expressed in cranial NC primordia marked by *foxd3* at 1S (Fig. 4I) and continues in the bilateral NC domains from which *zic2a* is excluded through 6S (Fig. 4J,K). In addition, *zic2b* expression extends into the posterior neural keel during early somitogenesis, while *zic2a* expression does not (Fig. 4L).

To determine if the zebrafish *zic2* genes regulate NC induction, we examined early NC marker expression in *zic2* morphants. *Sna1b* expression levels are unaffected in most *zic2a* morphants (77% of morphants, Fig. 4M,N), with only 23% of embryos showing a mild reduction in staining. Single knockdown of Zic2b reduced the expression of *sna1b* in 40% of morphant embryos and eliminated it in 34% of *zic2b* morphants (Fig. 4O), while depleting Zic2a and Zic2b together eliminated *sna1b* expression in most morphants (63%, not shown) and reduced the NC domain in 30% of morphant embryos (30%, Fig. 4P). Similar results were obtained by ISH for *sox9b* (data not shown). These data suggest that *zic2a* and *zic2b*

both contribute to the timely induction of the NC and that *zic2b*, whose expression persists longer in the NC, plays a more critical role.

We next asked if *Zic2* continues to regulate NC development after induction. In control 18hpf embryos, *sox10* expression marks the cranial NC cells, which have exited the neural tube and are migrating forward in bilateral streams (Fig. 5A). Injection of *zic2a*MO or *zic2b*MO singly resulted in accumulation of *sox10*-expressing cells on the dorsal aspect of the midbrain and hindbrain (Fig. 5B,C). A similar phenotype was observed in embryos injected with both *zic2a*MO and *zic2b*MO (Fig. 5D), indicating that both *zic2a* and *zic2b* functions contribute to the timely emigration of cranial NC. Importantly, *sox10* expression did not appear reduced in *zic2b* morphants, suggesting that cranial NC may recover after an initial delay in induction following *Zic2b* knockdown.

In contrast to *zic2* morphants, dorsal mislocalization of NC cells was not observed after elevation of *Zic2a* levels in transgenic overexpressors. Both YFP-negative siblings and embryos expressing *Zic2a*YFP after a 10hpf HS displayed wild-type localization of *sox10*-positive cells, despite the characteristic abnormal neural tube morphology in overexpressors (Fig. 5E,F). The number of *sox10*-positive cells increased in embryos expressing *Zic2a*YFP (Fig. 5F and Supplemental Fig. 2J,K), as did the overall amount of *sox10* transcript measured by quantitative real-time PCR (Fig. 5G), suggesting expansion in NC cells following *Zic2a* misexpression. Taken together, these data demonstrate important roles for *Zic2* in the timing of cranial NC induction and in neural tube exit and/or migratory onset, with *zic2b* playing a more prominent role in the process of induction.

### ***zic2a* and *zic2b* regulate pigment NC lineages**

In addition to cranial cartilage, the NC forms chromatophores, and defects in facial cartilage often correlate with pigment defects (Schilling et al., 1996). To test whether *Zic2* functions in pigment cell formation, we examined expression of several lineage-specific marker genes in *zic2a* and *zic2b* morphants. NC cells fated to differentiate into melanophores express the *mitfa* transcription factor at 24hpf (Fig. 6A). While knockdown of *Zic2a* alone caused only a mild reduction in *mitfa* staining, depletion of *Zic2b* resulted in a dramatic reduction of melanophore precursors in the trunk (Fig. 6B,C). Double *Zic2* knockdown extended the reduction of *mitfa* expression into the cranial region (Fig. 6D). These data indicate that *zic2b* is required to generate the appropriate number of melanophores in the trunk, while *zic2a* and *zic2b* work together to regulate melanophore development in the cranial region.

NC cells fated to become xanthophores express *gch2* at 24hpf (Fig. 6E). In contrast to *mitfa*, *gch2* expression was reduced at all axial levels of *zic2a* morphants (Fig. 6F). *Zic2b* depletion again preferentially reduced *gch2* expression in the trunk (Fig. 6G). Double knockdown caused a severe reduction of *gch2* expression in cranial and trunk regions, similar to single *Zic2a* depletion (Fig. 6H). Double morphants and *zic2b* single morphants had a distinctive phenotype in the cranial region, where NC cells formed large aggregates (asterisks in Fig. 6C,G). Additionally, many *Zic2b*-depleted embryos had aberrantly localized pigment cell precursors on the dorsal aspect of the neural tube (asterisk in C inset; see Fig. 5). Transverse sections through the midbrains of *gch2*-stained embryos revealed no difference between control embryos and *zic2a* morphants (Fig. 6I,J). However, *zic2b* morphants and double morphants exhibited large conglomerates of pigment cell precursors, which had exited the neural tube, but migrated abnormally (asterisks in Fig. 6K,L). In addition, some NC cells were extruded into the lumen from the apical surface, rather than exiting the basal side of the neural epithelium (arrow in Fig. 6L). Together, these results argue that *zic2a* and *zic2b* contribute to the regulation of chromatophore development and exit from the neural tube, with differing requirements at cranial and trunk axial levels.

## Zic2a and Zic2b functions contribute to the formation of pharyngeal arch primordia

NC-derived jaw precursors migrate from the hindbrain to colonize the pharyngeal arches during normal development (Schilling and Kimmel, 1994). Having shown that *zic2a* and *zic2b* help orchestrate the onset of cranial NC migration, we hypothesized that cells retained in or near the dorsal neural tube of *zic2* morphants are fated to contribute to specific NC-derived lineages, including pharyngeal arch primordia. Using *dlx2a* expression as a marker, we determined that migration of the NC cells to the first two pharyngeal arches, PA1 and PA2, remained largely unaltered in *zic2* morphants, since no dorsally mislocalized *dlx2a*-positive cells were observed (Fig. 7A–D). However, *dlx2a*-positive PA1 and PA2 were reduced in 30% of *zic2a* morphants (Fig. 7B). *Dlx2a* expression in the arches was unchanged in *zic2b* morphants (Fig. 7C). *Zic2* double knockdown caused a reduction in the size of PA1 and PA2 (33% of morphants), the posterior pharyngeal arches (24% of morphants, Fig. 7D), or all pharyngeal arches (22% of morphants).

To further probe the role of *Zic2* in PA formation, we induced expression of *Zic2a*YFP at several time points. After induction at 10hpf, mispatterning of *dlx2a* was observed in *Zic2a*YFP-positive embryos, consisting of an incomplete separation of PA1 and PA2 in 36% of overexpressors (Fig. 7E,F; arrow in 7F). After induction at 14hpf, pharyngeal arch *dlx2a* expression in *Zic2a*YFP-positive embryos was indistinguishable from that seen in controls (Fig. 7G,H), despite the fact that older siblings had severe and fully penetrant craniofacial defects at 5dpf (see Fig. 2). Collectively, these data argue that the pharyngeal cartilage defects in *zic2a* morphants and *Zic2a*YFP overexpressors may not be fully attributable to early defects in NC specification and migratory onset.

To test whether *zic2a* expression is required within the chondrogenic lineage to promote craniofacial cartilage development, we employed cell transplantation assays. Cells transplanted from control morphant donors to control morphant hosts contributed to both the pharyngeal cartilage (Fig. 7I, see arrowheads) and neurocranium (Fig. 7J, see arrowhead) (4/7 embryos, 1 exp., see asterisks in Supplemental Table 1). Similarly, *Zic2a*-depleted cells transplanted into control hosts contributed to the pharyngeal cartilages (Fig. 7K,K') and the neurocranium (Fig. 7L,L'), but somewhat less frequently than control cells (3/19 embryos, 2 exp., see asterisks in Supplemental Table 2). Control morphant cells transplanted to a *zic2a* morphant background also contributed to craniofacial cartilages, suggesting that *Zic2a* is not required in surrounding cartilage for integration (2/17 embryos, 1 exp., Supplemental Fig. 5 and Supplemental Table 4). Control cell integration into cartilages did not lead to appreciable rescue of the *Zic* morphant defect. We observed unusual left-right asymmetry of the host pharyngeal cartilage defects in several embryos (Supplemental Fig. 5D) This asymmetry was not observed in *Zic* morphants and is suggestive of non-autonomous rescue by control morphant cells when transplanted into tissues surrounding chondrogenic tissues. Due to a broad distribution of donor cells, we could not conclusively determine which surrounding tissue might be involved. Both control and *Zic2a*-depleted transplanted cells also contributed to NC lineages earlier during development, at 24hpf (asterisks in Supplemental Fig. 5 and Supplemental Tables 3,5).

Among wild-type embryos that received *Zic2*-morphant transplants, several embryos developed with defects in host-derived neurocranium (5/19, 2 exp., asterisks in Fig. 7L, Supplemental Table 2). All of these embryos had significant contributions of *Zic* morphant cells to adjacent forebrain, while control-to-control transplants showed no craniofacial cartilage defects (7/7, 1exp.). These observations argue against a strict cell-autonomous requirement for *Zic2a* function, but are consistent with a dual role for *Zic2* in the forebrain neuroepithelium and potentially in the chondrogenic NC itself.



## Zebrafish *Zic2* patterns the ventral forebrain primordium

The proximal environment of the post-migratory NC-derived chondrogenic precursors plays a key role in promoting NC condensation, proliferation and differentiation into cartilage (Szabo-Rogers et al., 2010). Since early defects in NC development may not fully explain the craniofacial anomalies in *Zic2*-depleted and misexpressing embryos, we hypothesized that *Zic2* patterns tissues surrounding the cartilages, and that incorrect signaling from these mispatterned tissues contributes to the craniofacial defects observed in embryos with disrupted *Zic2* levels. Consistent with this hypothesis, previous work in our lab showed that *zic2a* is required for diencephalic development and for modulating Hh signaling in the forebrain (Sanek et al., 2008; Sanek et al., 2009). To extend these studies, we examined forebrain patterning in *Zic2b*-depleted morphant embryos. A mild deficit in the prethalamal domain *dlx2a* was observed in 51% of the embryos (Fig. 8A,B, see arrowhead). The prethalamal defect was similar to, but less pronounced, than that seen in *zic2a* morphants (Fig. 8C, Sanek et al., 2007) or in *zic2* double morphants (Fig. 8D). The ventral midline of the forebrain primordium, marked by *ptch2* expression, was unaffected by *Zic2* depletion (Supp. Fig. 6). This mild forebrain mispatterning correlates with mild craniofacial cartilage defects in *zic2b* morphants (see Fig. 1).

To further test the correlation between early forebrain patterning deficits and late craniofacial defects, we used temporally controlled *Zic2a*YFP misexpression. Craniofacial cartilages are strongly affected by *Zic2* elevation after 10hpf and 14hpf heat-shocks, and much less so after 17hpf heat-shocks (Fig. 2). Similarly, we have found *dlx2a* expression to be disrupted in the telencephalon and diencephalon of 66% of *Zic2a*YFP overexpressors after induction at 10hpf (Fig. 8E,F) and in 39% after induction 14 hpf (data not shown). Importantly, ectopic *Zic2a* expression following a 17hpf heat shock did not cause forebrain patterning defects (data not shown). Together, these data provide correlative support to the hypothesis that aberrantly formed ventral forebrain may contribute to craniofacial deficits in embryos with reduced or elevated *Zic2* levels.

Expression of *ptch2*, a critical component and target of Hh signaling (Concordet et al., 1996), was strongly reduced in the ventral midline of the entire brain primordium after *Zic2a*YFP induction at 10hpf (Fig. 8G,H). Despite this global reduction, expression was maintained in the ZLI, the main source of Hh signaling in the diencephalon (Scholpp et al., 2006). Similarly, expression of *nkx2.2a*, another target of Hh signaling (Barth and Wilson, 1995), was reduced in the ventral midline of the hindbrain (Fig. 8I, J). Thus, the ventral midline of the brain primordium is aberrantly formed upon *Zic2a*YFP induction, and is likely compromised in its ability to signal to adjacent tissues, under the same experimental conditions that lead to profound craniofacial defects. Notably, the oropharyngeal epithelium, another important source of morphogens during craniofacial development, is mispatterned in *zic2a*-depleted and misexpressing embryos (Fig. 8K,L and Supplemental Fig. 7). However, this mispatterning is observed later during development only in strongly affected morphants, and may be a consequence of earlier defects in the neuroepithelium. Collectively, these data demonstrate an early role for both *Zic2a* and *Zic2b* in patterning the ventral brain primordium that likely contributes to their roles in craniofacial development.

## Discussion

*Zic2*, a highly conserved transcription factor with essential functions during mammalian brain development, is encoded by two genes in the zebrafish genome, *zic2a* and *zic2b*. Data presented here identify a novel requirement for *Zic2* during craniofacial development in zebrafish. We show that the forming jaw and neurocranium are sensitive to artificial elevation of *Zic2* levels prior to 24hpf, suggesting an early role for *Zic2* in craniofacial development. Since the craniofacial skeleton is largely derived from the NC, we have

examined the relative contributions of the two *Zic2* orthologs to neural crest formation. We show that *Zic2a* and *Zic2b* regulate several aspects of neural crest development, including induction and migratory onset of the pigment lineages, and generation and proper organization of pre-chondrogenic NC that contribute to pharyngeal primordia. Correct morphogenesis of craniofacial cartilages relies on signals from the adjacent neural epithelium where *Zic2* plays an important role that likely contributes to its overall function during craniofacial development.

### **Zic2 and craniofacial development**

We have shown that in the zebrafish craniofacial cartilages are disrupted following depletion of the *ZIC2* orthologs *zic2a* and *zic2b*, products of the teleost genome duplication that share an 82.5% amino acid identity with each other (Meyer and Van de Peer, 2005; Toyama et al., 2004; Vandepoele et al., 2004). This phenotype is consistent with craniofacial abnormalities in mouse mutants of *Zic5*, which is co-expressed and co-regulated with *Zic2* (Inoue et al., 2004). Craniofacial defects have not been reported in *Zic2* knockout mice, which die during gestation (Elms et al., 2003; Warr et al., 2008); however, human patients with *ZIC2*-associated holoprosencephaly exhibit a characteristic set of mild craniofacial dysmorphologies (Solomon et al., 2010a). Collectively, these observations indicate an evolutionarily conserved role for *Zic2* during craniofacial development, the mechanism of which remains to be explored.

The incompletely penetrant reduction of the NC-derived pharyngeal arches in *Zic2a*-depleted zebrafish embryos is consistent with early NC deficits reported in *Zic2* and *Zic5* mouse mutants (Elms et al., 2003; Inoue et al., 2004; Nagai et al., 2000). However, several lines of evidence argue that these NC deficits do not completely account for the severe craniofacial defects seen in zebrafish embryos with reduced and enhanced levels of *Zic2*. First, we have demonstrated that *zic2b* plays a more prominent role than *zic2a* in NC induction, while *zic2a* is more critical for craniofacial development. Second, *zic2a* and *zic2b* are expressed in the brain primordium, but not in the pharyngeal arches or the adjacent stomodeum and craniofacial mesenchyme. Third, we have shown that transplanted *Zic2a*-deficient cells can contribute to migrating NC and to differentiated craniofacial cartilages in a wild-type background, suggesting that *Zic2a* is not strictly required in the NC-derived chondrogenic lineage. Additionally, our transplant data suggest that defects in host-derived neurocranium (i.e. abnormal trabeculae) are correlated with clusters of *Zic2a*-depleted transplanted cells in the adjacent ventral forebrain. These data, while not conclusive, are consistent with the hypothesis that *Zic2* controls the developing craniofacial cartilages in part via its role in patterning the forebrain.

In support of this hypothesis, we have shown that depletion of *Zic2a* or *Zic2b*, or misexpression of *Zic2a*, lead to mispatterning of the ventral midline of the brain primordium, as well as to craniofacial defects. The timing of heat shock induction experiments shows that craniofacial cartilages are sensitive to disruption by *Zic2a* relatively early, prior to 24hpf. Ventral forebrain signaling occurring around 10hpf is required to pattern the zebrafish oral ectoderm (stomodeum) in preparation for the arrival of chondrogenic NC (Eberhart et al., 2006). Intriguingly, the pharyngeal epithelium is mispatterned in *Zic2a*-depleted embryos, suggesting the possibility that it is compromised in its ability to support differentiation of chondrogenic precursors.

We have also demonstrated a role for *Zic2a* in the forming optic stalk (see Supplemental Fig. 2; Sanek et al., 2009), which could contribute to its influence over craniofacial development. The retina and optic stalk are sources of several morphogens with roles in craniofacial development such as PDGF, RA, and Shh (Eberhart et al., 2008; Kish et al., 2011). It has been suggested that the eye is critical for directing neural crest migration, and

may secrete positive cues for NC cells migrating towards the most anterior neurocranial structures, e.g. the ethmoid plate (Langenberg et al., 2008). In mouse (Brown et al., 2003) and zebrafish, *Zic2* is expressed in the optic stalks, and regulates patterning of the retina/optic stalk interface and the adjacent ventral forebrain (Sanek et al., 2009). Compared with the well-supported roles for neural, ectodermal and endodermal signaling centers, little is known about the eye and optic stalk as organizers of NC migration and craniofacial development. Our ongoing efforts to identify optic stalk-specific targets of *Zic2a* will shed light on the manner in which these tissues contribute to craniofacial morphogenesis.

Early signaling by *Shh*, one of the key growth factors produced by the ventral midline of the brain primordium (Chiang et al., 1996), controls cell identity and patterning in surrounding tissues (Ingham and Placzek, 2006). Notably, *SHH* is the most commonly mutated gene in HPE patients (Roessler et al., 1996). We have previously shown that *Zic2a* is a negative regulator of gene expression downstream of Hh signaling (Sanek et al., 2008; Sanek et al., 2009), and hypothesize that *Zic2a* interacts with the Hh signaling pathway to regulate patterning of the neural and oropharyngeal epithelia, which subsequently affects craniofacial development. Consistent with this hypothesis, we find that *Zic2a*YFP overexpression inhibits expression of the Hh signaling target *ptch2*, and that *Zic2a*YFP overexpressors develop with craniofacial defects similar to those caused by Hh abrogation in zebrafish, namely, hypoplastic pharyngeal cartilages, lack of medial ethmoid plate, and fused trabeculae (Wada et al., 2005; Schwend and Ahlgren, 2009; Swartz et al., 2012).

Fgf and Wnt signaling pathways interact with *Zics* and play important roles in craniofacial development. Fgf signaling regulates *zic5* expression in *Xenopus* (Monsoro-Burq et al., 2003) and interacts with *Zic2a* during zebrafish optic stalk development (Sanek et al., 2009), and zebrafish *fgf8* mutants develop with craniofacial defects (Albertson and Yelick, 2005). Zebrafish *zic2a* and *zic5* are direct targets of Wnt signaling, which regulates outgrowth of chondrogenic structures (Nyholm et al., 2007; Reid et al., 2011). To fully understand the role of *zic* genes in craniofacial development, it will be important to determine how *Zic2* interacts with these signaling pathways.

### **Zic2 and neural crest development**

*Zic* genes function at the border of the neural plate to specify NC identity (Brewster et al., 1998; Hong and Saint-Jeannet, 2007; Sato et al., 2005), and *Zic2* is required for generation of the appropriate number of NC cells in mice (Elms et al., 2003). In zebrafish, *zic2a* and *zic2b* are largely co-expressed, except in the early NC, which expresses only *zic2b*. This study represents the first analysis of *zic2b* function in zebrafish, and establishes its role in several aspects of NC development, including NC induction and pigment lineage development.

NC cells undergo comprehensive changes in morphology and adhesion as they exit the basal surface of the neural tube and begin migrating throughout the embryo (Theveneau and Mayor, 2012; Clay and Halloran, 2011). In zebrafish *zic2* morphants, we observe distinct defects during this phase of NC development. These include failure to initiate migration away from the neural tube and extrusion of NC cells into the neural tube lumen. There are several mechanisms by which the *zic2* genes may contribute to these aspects of NC development. Canonical Wnt signaling is important during several phases of neural crest development, including induction (Garcia-Castro et al., 2002; Patthey et al., 2009; Steventon et al., 2009), proliferation (Dickinson et al., 1994; Ikeya et al., 1997; Megason and McMahon, 2002) and delamination (Burstyn-Cohen et al., 2004). Our lab has shown that *zic2a* is a direct target of Wnt signaling, and itself promotes proliferation in the dorsal midbrain (Nyholm et al., 2007). A recent report showed that *Xenopus* *Zic3* protein suppresses the Wnt/ $\beta$ -catenin signaling pathway (Fujimi et al., 2011). In cell culture, human

ZIC2 protein can interact directly with Tcf4 and act as a negative regulator of Wnt signaling (Pourebrahim et al., 2011). Since it is unclear when and in which tissues these interactions occur *in vivo*, it will be important to examine the interaction between Zics and Wnt signaling in the dorsal neural tube, and during NC induction and proliferation.

Canonical Wnt signaling also promotes the specification of pigment cells from within the NC population. *Wnt1/Wnt3a* null mice have very depleted pigment cell populations (Ikeya et al., 1997). In zebrafish, Wnt signaling promotes pigment cell formation at the expense of other NC-derived cell types, such as neurons (Dorsky et al., 1998). Both *zic2a* and *zicb* promote development of melanophores and xanthophores in the cranial region. In the trunk, *Zic2b* acts without contribution from *Zic2a* to regulate pigment cell development. It will be interesting to test whether either or both *zic2* genes interact with the Wnt signaling pathway to regulate the specification of the pigment cell lineages.

Finally, *zic2a* and *zic2b* may regulate adhesion in the dorsal brain. Concomitant depletion of *Zic2a* and *Zic2b* causes large aggregations of NC cells to accumulate. Eph/ephrin signaling regulates adhesion in epithelial cells (Dahmann et al., 2011; Pasquale et al., 2005) and is important during NC migration (Kuriyama and Mayor, 2008; Santiago and Erickson, 2002). *Zic2* regulates the expression of EphB1 in the mouse forebrain (Garcia-Frigola et al., 2008; Lee et al., 2008) and *Zic2a* regulates several zebrafish ephrins expressed in the dorsal brain (J.T. and M.N., unpublished observations). Wnt signaling regulates changes in cell adhesion that occur in delaminating NC cells through one of its targets, the zinc-finger transcription factor *ovo1* (Piloto and Schilling, 2010). Given that *zic2a* is also a target of Wnt signaling, it will be important to determine if *Zic2* plays a role in regulating the adhesive properties of the dorsal neural tube from which chondrogenic NC cells exit.

### Using zebrafish to dissect Zic functions during brain and craniofacial development

How brain and craniofacial morphogenesis are coordinated remains an important outstanding question in developmental biology. The etiologies of brain defects such as HPE and DWM are complex, seldom attributable to a single genetic alteration (Schachter and Krauss, 2008; Solomon et al., 2010b), and the relationship between the neural and craniofacial phenotypes associated with these diseases is not clear. *Zic* genes are key regulators of both brain and craniofacial development: in mammals, reduced *Zic2* levels are causally associated with gross morphological disruptions of forebrain development (HPE) and facial dysmorphology. The closely related *ZIC1* and *ZIC4* are linked to DWM, a congenital syndrome characterized by cerebellar hypoplasia, as well as craniofacial dysmorphologies reminiscent of those observed in *ZIC2*-associated HPE patients (Grinberg et al., 2004; Blank et al., 2011). Moreover, *ZIC2* mutations have been identified in a patient with DWM (Mademont-Soler et al., 2010). Having determined the relative contributions of *Zic2a* and *Zic2b* to forebrain and craniofacial development in zebrafish, we are positioned to answer two important outstanding questions: (1) In which tissues do vertebrate *Zics* function? and (2) what is the mechanism of their function? These questions will be addressed in future studies through tissue-specific manipulation of *Zic* function, identification and functional analysis of *Zic* transcriptional targets, and identification of genetic modifiers of *Zic* function in zebrafish.

### Supplementary Material

Refer to Web version on PubMed Central for supplementary material.

## Acknowledgments

We thank Eric Pueschel, Nick Sanek, Jingzhu (Michael) Zhang, Matt Clay and Mary Halloran for valuable discussions throughout the course of this work, Sreelaja Nair for technical advice and Mike Padilla for expert help. We are grateful to Mary Halloran, Bruce Appel, Becky Burdine, Michael Nonet and the Zebrafish International Resource Center for fish lines and plasmids, and Tony Stretton for sharing equipment. This work was funded by grants from NIH and the American Heart Association to Y.G.

## References

- Ahlgren SC, Bronner-Fraser M. Inhibition of sonic hedgehog signaling in vivo results in craniofacial neural crest cell death. *Curr Biol*. 1999; 9:1304–14. [PubMed: 10574760]
- Akimenko MA, Ekker M, Wegner J, Lin W, Westerfield M. Combinatorial expression of three zebrafish genes related to distal-less: part of a homeobox gene code for the head. *J Neurosci*. 1994; 14:3475–86. [PubMed: 7911517]
- Albertson RC, Yelick PC. Roles for fgf8 signaling in left-right patterning of the visceral organs and craniofacial skeleton. *Dev Biol*. 2005; 283:310–21. [PubMed: 15932752]
- Barrallo-Gimeno A, Holzschuh J, Driever W, Knapik EW. Neural crest survival and differentiation in zebrafish depends on mont blanc/tfap2a gene function. *Development*. 2004; 131:1463–77. [PubMed: 14985255]
- Barth KA, Wilson SW. Expression of zebrafish nk2.2 is influenced by sonic hedgehog/vertebrate hedgehog-1 and demarcates a zone of neuronal differentiation in the embryonic forebrain. *Development*. 1995; 121:1755–68. [PubMed: 7600991]
- Blank MC, Grinberg I, Aryee E, Laliberte C, Chizhikov VV, Henkelman RM, Millen KJ. Multiple developmental programs are altered by loss of Zic1 and Zic4 to cause Dandy-Walker malformation cerebellar pathogenesis. *Development*. 2011; 138:1207–16. [PubMed: 21307096]
- Bonilla-Claudio M, Wang J, Bai Y, Klysik E, Selever J, Martin JF. Bmp signaling regulates a dose-dependent transcriptional program to control facial skeletal development. *Development*. 2012; 139:709–19. [PubMed: 22219353]
- Brewster R, Lee J, Ruiz i Altaba A. Gli/Zic factors pattern the neural plate by defining domains of cell differentiation. *Nature*. 1998; 393:579–83. [PubMed: 9634234]
- Brown LY, Kottmann AH, Brown S. Immunolocalization of Zic2 expression in the developing mouse forebrain. *Gene Expr Patterns*. 2003; 3:361–7. [PubMed: 12799086]
- Brown SA, Warburton D, Brown LY, Yu CY, Roeder ER, Stengel-Rutkowski S, Hennekam RC, Muenke M. Holoprosencephaly due to mutations in ZIC2, a homologue of *Drosophila* odd-paired. *Nat Genet*. 1998; 20:180–3. [PubMed: 9771712]
- Burstyn-Cohen T, Stanleigh J, Sela-Donenfeld D, Kalcheim C. Canonical Wnt activity regulates trunk neural crest delamination linking BMP/noggin signaling with G1/S transition. *Development*. 2004; 131:5327–39. [PubMed: 15456730]
- Chiang C, Litingtung Y, Lee E, Young KE, Corden JL, Westphal H, Beachy PA. Cyclopia and defective axial patterning in mice lacking Sonic hedgehog gene function. *Nature*. 1996; 383:407–13. [PubMed: 8837770]
- Chong HJ, Young NM, Hu D, Jeong J, McMahon AP, Hallgrímsson B, Marcucio RS. Signaling by SHH rescues facial defects following blockade in the brain. *Dev Dyn*. 2012; 241:247–56. [PubMed: 22275045]
- Clay MR, Halloran MC. Regulation of cell adhesions and motility during initiation of neural crest migration. *Curr Opin Neurobiol*. 2011; 21:17–22. [PubMed: 20970990]
- Concordet JP, Lewis KE, Moore JW, Goodrich LV, Johnson RL, Scott MP, Ingham PW. Spatial regulation of a zebrafish patched homologue reflects the roles of sonic hedgehog and protein kinase A in neural tube and somite patterning. *Development*. 1996; 122:2835–46. [PubMed: 8787757]
- Cordero DR, Brugmann S, Chu Y, Bajpai R, Jame M, Helms JA. Cranial neural crest cells on the move: their roles in craniofacial development. *Am J Med Genet A*. 2011; 155A:270–9. [PubMed: 21271641]

- Couly G, Creuzet S, Bennaceur S, Vincent C, Le Douarin NM. Interactions between Hox-negative cephalic neural crest cells and the foregut endoderm in patterning the facial skeleton in the vertebrate head. *Development*. 2002; 129:1061–73. [PubMed: 11861488]
- Cresko WA, Yan YL, Baltrus DA, Amores A, Singer A, Rodriguez-Mari A, Postlethwait JH. Genome duplication, subfunction partitioning, and lineage divergence: Sox9 in stickleback and zebrafish. *Dev Dyn*. 2003; 228:480–9. [PubMed: 14579386]
- Dahmann C, Oates AC, Brand M. Boundary formation and maintenance in tissue development. *Nat Rev Genet*. 2011; 12:43–55. [PubMed: 21164524]
- Dickinson ME, Krumlauf R, McMahon AP. Evidence for a mitogenic effect of Wnt-1 in the developing mammalian central nervous system. *Development*. 1994; 120:1453–71. [PubMed: 8050356]
- Dorsky RI, Moon RT, Raible DW. Control of neural crest cell fate by the Wnt signalling pathway. *Nature*. 1998; 396:370–3. [PubMed: 9845073]
- Dubourg C, Bendavid C, Pasquier L, Henry C, Odent S, David V. Holoprosencephaly. *Orphanet J Rare Dis*. 2007; 2:8. [PubMed: 17274816]
- Dutton KA, Pauliny A, Lopes SS, Elworthy S, Carney TJ, Rauch J, Geisler R, Haffter P, Kelsh RN. Zebrafish colourless encodes sox10 and specifies non-ectomesenchymal neural crest fates. *Development*. 2001; 128:4113–25. [PubMed: 11684650]
- Eberhart JK, He X, Swartz ME, Yan YL, Song H, Boling TC, Kunerth AK, Walker MB, Kimmel CB, Postlethwait JH. MicroRNA Mirn140 modulates Pdgf signaling during palatogenesis. *Nat Genet*. 2008; 40:290–8. [PubMed: 18264099]
- Eberhart JK, Swartz ME, Crump JG, Kimmel CB. Early Hedgehog signaling from neural to oral epithelium organizes anterior craniofacial development. *Development*. 2006; 133:1069–77. [PubMed: 16481351]
- Elms P, Siggers P, Napper D, Greenfield A, Arkell R. Zic2 is required for neural crest formation and hindbrain patterning during mouse development. *Dev Biol*. 2003; 264:391–406. [PubMed: 14651926]
- Essner JJ, Branford WW, Zhang J, Yost HJ. Mesendoderm and left-right brain, heart and gut development are differentially regulated by pitx2 isoforms. *Development*. 2000; 127:1081–93. [PubMed: 10662647]
- Fujimi TJ, Hatayama M, Aruga J. Xenopus Zic3 controls notochord and organizer development through suppression of the Wnt/beta-catenin signaling pathway. *Dev Biol*. 2012; 361:220–31. [PubMed: 22056782]
- Garcia-Castro MI, Marcelle C, Bronner-Fraser M. Ectodermal Wnt function as a neural crest inducer. *Science*. 2002; 297:848–51. [PubMed: 12161657]
- Garcia-Frigola C, Carreres MI, Vegar C, Mason C, Herrera E. Zic2 promotes axonal divergence at the optic chiasm midline by EphB1-dependent and -independent mechanisms. *Development*. 2008; 135:1833–41. [PubMed: 18417618]
- Gillhouse M, Wagner Nyholm M, Hikasa H, Sokol SY, Grinblat Y. Two Frodo/Dapper homologs are expressed in the developing brain and mesoderm of zebrafish. *Dev Dyn*. 2004; 230:403–9. [PubMed: 15188426]
- Grinberg I, Northrup H, Ardinger H, Prasad C, Dobyns WB, Millen KJ. Heterozygous deletion of the linked genes ZIC1 and ZIC4 is involved in Dandy-Walker malformation. *Nat Genet*. 2004; 36:1053–5. [PubMed: 15338008]
- Grinblat Y, Sive H. zic Gene expression marks anteroposterior pattern in the presumptive neurectoderm of the zebrafish gastrula. *Dev Dyn*. 2001; 222:688–93. [PubMed: 11748837]
- Haworth KE, Wilson JM, Grevellec A, Cobourne MT, Healy C, Helms JA, Sharpe PT, Tucker AS. Sonic hedgehog in the pharyngeal endoderm controls arch pattern via regulation of Fgf8 in head ectoderm. *Dev Biol*. 2007; 303:244–58. [PubMed: 17187772]
- Hong CS, Saint-Jeannet JP. The activity of Pax3 and Zic1 regulates three distinct cell fates at the neural plate border. *Mol Biol Cell*. 2007; 18:2192–202. [PubMed: 17409353]
- Hoyle J, Tang YP, Wiertel EL, Wardle FC, Sive H. nlz gene family is required for hindbrain patterning in the zebrafish. *Dev Dyn*. 2004; 229:835–46. [PubMed: 15042707]

- Hu D, Marcucio RS. A SHH-responsive signaling center in the forebrain regulates craniofacial morphogenesis via the facial ectoderm. *Development*. 2009; 136:107–16. [PubMed: 19036802]
- Ikeya M, Lee SM, Johnson JE, McMahon AP, Takada S. Wnt signalling required for expansion of neural crest and CNS progenitors. *Nature*. 1997; 389:966–70. [PubMed: 9353119]
- Inbal A, Kim SH, Shin J, Solnica-Krezel L. Six3 represses nodal activity to establish early brain asymmetry in zebrafish. *Neuron*. 2007; 55:407–415. [PubMed: 17678854]
- Ingham PW, Placzek M. Orchestrating ontogenesis: variations on a theme by sonic hedgehog. *Nat Rev Genet*. 2006; 7:841–50. [PubMed: 17047684]
- Inoue T, Hatayama M, Tohmonda T, Itohara S, Aruga J, Mikoshiba K. Mouse *Zic5* deficiency results in neural tube defects and hypoplasia of cephalic neural crest derivatives. *Dev Biol*. 2004; 270:146–62. [PubMed: 15136147]
- Jeong J, Mao J, Tenzen T, Kottmann AH, McMahon AP. Hedgehog signaling in the neural crest cells regulates the patterning and growth of facial primordia. *Genes Dev*. 2004; 18:937–51. [PubMed: 15107405]
- Karlstrom RO, Tyurina OV, Kawakami A, Nishioka N, Talbot WS, Sasaki H, Schier AF. Genetic analysis of zebrafish *gli1* and *gli2* reveals divergent requirements for *gli* genes in vertebrate development. *Development*. 2003; 130:1549–64. [PubMed: 12620981]
- Kawakami K, Takeda H, Kawakami N, Kobayashi M, Matsuda N, Mishina M. A transposon-mediated gene trap approach identifies developmentally regulated genes in zebrafish. *Developmental Cell*. 2004; 7:133–144. [PubMed: 15239961]
- Kimmel CB, Ballard WW, Kimmel SR, Ullmann B, Schilling TF. Stages of embryonic development of the zebrafish. *Dev Dyn*. 1995; 203:253–310. [PubMed: 8589427]
- Kimmel CB, Miller CT, Kruze G, Ullmann B, BreMiller RA, Larison KD, Snyder HC. The shaping of pharyngeal cartilages during early development of the zebrafish. *Dev Biol*. 1998; 203:245–63. [PubMed: 9808777]
- Kish PE, Bohnsack BL, Gallina D, Kasprick DS, Kahana A. The eye as an organizer of craniofacial development. *Genesis*. 2011; 49:222–30. [PubMed: 21309065]
- Knight RD, Nair S, Nelson SS, Afshar A, Javidan Y, Geisler R, Rauch GJ, Schilling TF. *lockjaw* encodes a zebrafish *tfap2a* required for early neural crest development. *Development*. 2003; 130:5755–68. [PubMed: 14534133]
- Kuriyama S, Mayor R. Molecular analysis of neural crest migration. *Philos Trans R Soc Lond B Biol Sci*. 2008; 363:1349–62. [PubMed: 18198151]
- Langenberg T, Kahana A, Wszalek JA, Halloran MC. The eye organizes neural crest cell migration. *Dev Dyn*. 2008; 237:1645–52. [PubMed: 18498099]
- Le Douarin NM, Couly G, Creuzet SE. The neural crest is a powerful regulator of pre-otic brain development. *Dev Biol*. 2012; 366:74–82. [PubMed: 22269168]
- Lee R, Petros TJ, Mason CA. *Zic2* regulates retinal ganglion cell axon avoidance of ephrinB2 through inducing expression of the guidance receptor EphB1. *J Neurosci*. 2008; 28:5910–9. [PubMed: 18524895]
- Li W, Cornell RA. Redundant activities of *Tfap2a* and *Tfap2c* are required for neural crest induction and development of other non-neural ectoderm derivatives in zebrafish embryos. *Dev Biol*. 2007; 304:338–354. [PubMed: 17258188]
- Lister JA, Robertson CP, Lepage T, Johnson SL, Raible DW. *nacre* encodes a zebrafish microphthalmia-related protein that regulates neural-crest-derived pigment cell fate. *Development*. 1999; 126:3757–67. [PubMed: 10433906]
- Lumsden A, Sprawson N, Graham A. Segmental origin and migration of neural crest cells in the hindbrain region of the chick embryo. *Development*. 1991; 113:1281–91. [PubMed: 1811942]
- Mademont-Soler I, Morales C, Armengol L, Soler A, Sanchez A. Description of the smallest critical region for Dandy-Walker malformation in chromosome 13 in a girl with a cryptic deletion related to t(6;13)(q23;q32). *Am J Med Genet A*. 2010; 152A:2308–12. [PubMed: 20683983]
- Marcucio RS, Cordero DR, Hu D, Helms JA. Molecular interactions coordinating the development of the forebrain and face. *Dev Biol*. 2005; 284:48–61. [PubMed: 15979605]
- Marcucio RS, Young NM, Hu D, Hallgrímsson B. Mechanisms that underlie co-variation of the brain and face. *Genesis*. 2011; 49:177–89. [PubMed: 21381182]

- Maurus D, Harris WA. Zic-associated holoprosencephaly: zebrafish Zic1 controls midline formation and forebrain patterning by regulating Nodal, Hedgehog, and retinoic acid signaling. *Genes Dev.* 2009; 23:1461–73. [PubMed: 19528322]
- Megason SG, McMahon AP. A mitogen gradient of dorsal midline Wnts organizes growth in the CNS. *Development.* 2002; 129:2087–98. [PubMed: 11959819]
- Mercier S, Dubourg C, Garcelon N, Campillo-Gimenez B, Gicquel I, Belleguic M, Ratie L, Pasquier L, Loget P, Bendavid C, Jaillard S, Rochard L, Quelin C, Dupe V, David V, Odent S. New findings for phenotype-genotype correlations in a large European series of holoprosencephaly cases. *J Med Genet.* 2011; 48:752–60. [PubMed: 21940735]
- Merzdorf CS. Emerging roles for zic genes in early development. *Dev Dyn.* 2007; 236:922–40. [PubMed: 17330889]
- Meyer A, Van de Peer Y. From 2R to 3R: evidence for a fish-specific genome duplication (FSGD). *Bioessays.* 2005; 27:937–45. [PubMed: 16108068]
- Milet C, Monsoro-Burq AH. Neural crest induction at the neural plate border in vertebrates. *Dev Biol.* 2012; 366:22–33. [PubMed: 22305800]
- Minoux M, Rijli FM. Molecular mechanisms of cranial neural crest cell migration and patterning in craniofacial development. *Development.* 2010; 137:2605–21. [PubMed: 20663816]
- Monsoro-Burq AH, Fletcher RB, Harland RM. Neural crest induction by paraxial mesoderm in *Xenopus* embryos requires FGF signals. *Development.* 2003; 130:3111–24. [PubMed: 12783784]
- Nagai T, Aruga J, Minowa O, Sugimoto T, Ohno Y, Noda T, Mikoshiba K. Zic2 regulates the kinetics of neurulation. *Proc Natl Acad Sci U S A.* 2000; 97:1618–23. [PubMed: 10677508]
- Nakata K, Koyabu Y, Aruga J, Mikoshiba K. A novel member of the *Xenopus* Zic family, Zic5, mediates neural crest development. *Mech Dev.* 2000; 99:83–91. [PubMed: 11091076]
- Nakata K, Nagai T, Aruga J, Mikoshiba K. *Xenopus* Zic family and its role in neural and neural crest development. *Mech Dev.* 1998; 75:43–51. [PubMed: 9739105]
- Nasevicius A, Ekker SC. Effective targeted gene ‘knockdown’ in zebrafish. *Nat Genet.* 2000; 26:216–20. [PubMed: 11017081]
- Nie S, Kee Y, Bronner-Fraser M. Myosin-X is critical for migratory ability of *Xenopus* cranial neural crest cells. *Dev Biol.* 2009; 335:132–42. [PubMed: 19712673]
- Nyholm MK, Abdelilah-Seyfried S, Grinblat Y. A novel genetic mechanism regulates dorsolateral hinge-point formation during zebrafish cranial neurulation. *J Cell Sci.* 2009; 122:2137–48. [PubMed: 19470582]
- Nyholm MK, Wu SF, Dorsky RI, Grinblat Y. The zebrafish zic2a-zic5 gene pair acts downstream of canonical Wnt signaling to control cell proliferation in the developing tectum. *Development.* 2007; 134:735–46. [PubMed: 17215296]
- Odenthal J, Nusslein-Volhard C. fork head domain genes in zebrafish. *Dev Genes Evol.* 1998; 208:245–58. [PubMed: 9683740]
- Parichy DM, Ransom DG, Paw B, Zon LI, Johnson SL. An orthologue of the kit-related gene *fms* is required for development of neural crest-derived xanthophores and a subpopulation of adult melanocytes in the zebrafish, *Danio rerio*. *Development.* 2000; 127:3031–44. [PubMed: 10862741]
- Pasquale EB. Eph receptor signalling casts a wide net on cell behaviour. *Nat Rev Mol Cell Biol.* 2005; 6:462–75. [PubMed: 15928710]
- Patthey C, Edlund T, Gunhaga L. Wnt-regulated temporal control of BMP exposure directs the choice between neural plate border and epidermal fate. *Development.* 2009; 136:73–83. [PubMed: 19060333]
- Piloto S, Schilling TF. Ovo1 links Wnt signaling with N-cadherin localization during neural crest migration. *Development.* 2010; 137:1981–90. [PubMed: 20463035]
- Pourebahim R, Houtmeyers R, Ghogomu S, Janssens S, Thelie A, Tran HT, Langenberg T, Vleminckx K, Bellefroid E, Cassiman JJ, Tejpar S. Transcription factor Zic2 inhibits Wnt/beta-catenin protein signaling. *J Biol Chem.* 2011; 286:37732–40. [PubMed: 21908606]
- Reid BS, Yang H, Melvin VS, Taketo MM, Williams T. Ectodermal Wnt/beta-catenin signaling shapes the mouse face. *Dev Biol.* 2011; 349:261–9. [PubMed: 21087601]



- Roessler E, Belloni E, Gaudenz K, Jay P, Berta P, Scherer SW, Tsui LC, Muenke M. Mutations in the human Sonic Hedgehog gene cause holoprosencephaly. *Nat Genet.* 1996; 14:357–60. [PubMed: 8896572]
- Sanek NA, Grinblat Y. A novel role for zebrafish *zic2a* during forebrain development. *Dev Biol.* 2008; 317:325–35. [PubMed: 18358464]
- Sanek NA, Taylor AA, Nyholm MK, Grinblat Y. Zebrafish *zic2a* patterns the forebrain through modulation of Hedgehog-activated gene expression. *Development.* 2009; 136:3791–800. [PubMed: 19855021]
- Santiago A, Erickson CA. Ephrin-B ligands play a dual role in the control of neural crest cell migration. *Development.* 2002; 129:3621–32. [PubMed: 12117812]
- Sato T, Sasai N, Sasai Y. Neural crest determination by co-activation of *Pax3* and *Zic1* genes in *Xenopus* ectoderm. *Development.* 2005; 132:2355–63. [PubMed: 15843410]
- Schachter KA, Krauss RS. Murine models of holoprosencephaly. *Curr Top Dev Biol.* 2008; 84:139–70. [PubMed: 19186244]
- Schilling TF, Kimmel CB. Segment and cell type lineage restrictions during pharyngeal arch development in the zebrafish embryo. *Development.* 1994; 120:483–94. [PubMed: 8162849]
- Schilling TF, Kimmel CB. Musculoskeletal patterning in the pharyngeal segments of the zebrafish embryo. *Development.* 1997; 124:2945–60. [PubMed: 9247337]
- Schilling TF, Piotrowski T, Grandel H, Brand M, Heisenberg CP, Jiang YJ, Beuchle D, Hammerschmidt M, Kane DA, Mullins MC, van Eeden FJ, Kelsh RN, Furutani-Seiki M, Granato M, Haffter P, Odenthal J, Warga RM, Trowe T, Nusslein-Volhard C. Jaw and branchial arch mutants in zebrafish I: branchial arches. *Development.* 1996; 123:329–44. [PubMed: 9007253]
- Scholpp S, Wolf O, Brand M, Lumsden A. Hedgehog signalling from the zona limitans intrathalamica orchestrates patterning of the zebrafish diencephalon. *Development.* 2006; 133:855–64. [PubMed: 16452095]
- Schwend T, Ahlgren SC. Zebrafish *con/displ* reveals multiple spatiotemporal requirements for Hedgehog-signaling in craniofacial development. *BMC Dev Biol.* 2009; 9:59. [PubMed: 19948063]
- Solomon BD, Lacbawan F, Mercier S, Clegg NJ, Delgado MR, Rosenbaum K, Dubourg C, David V, Olney AH, Wehner LE, Hehr U, Bale S, Paulussen A, Smeets HJ, Hardisty E, Tylki-Szymanska A, Pronicka E, Clemens M, McPherson E, Hennekam RC, Hahn J, Stashinko E, Levey E, Wiczorek D, Roeder E, Schell-Apacik CC, Booth CW, Thomas RL, Kenwick S, Cummings DA, Bous SM, Keaton A, Balog JZ, Hadley D, Zhou N, Long R, Velez JI, Pineda-Alvarez DE, Odent S, Roessler E, Muenke M. Mutations in *ZIC2* in human holoprosencephaly: description of a novel *ZIC2* specific phenotype and comprehensive analysis of 157 individuals. *J Med Genet.* 2010; 47:513–24. [PubMed: 19955556]
- Solomon BD, Mercier S, Velez JI, Pineda-Alvarez DE, Wyllie A, Zhou N, Dubourg C, David V, Odent S, Roessler E, Muenke M. Analysis of genotype-phenotype correlations in human holoprosencephaly. *Am J Med Genet C Semin Med Genet.* 2010b; 154C:133–41. [PubMed: 20104608]
- Sperber SM, Saxena V, Hatch G, Ekker M. Zebrafish *dlx2a* contributes to hindbrain neural crest survival, is necessary for differentiation of sensory ganglia and functions with *dlx1a* in maturation of the arch cartilage elements. *Dev Biol.* 2008; 314:59–70. [PubMed: 18158147]
- Steventon B, Araya C, Linker C, Kuriyama S, Mayor R. Differential requirements of BMP and Wnt signalling during gastrulation and neurulation define two steps in neural crest induction. *Development.* 2009; 136:771–9. [PubMed: 19176585]
- Swartz ME, Nguyen V, McCarthy NQ, Eberhart JK. Hh signaling regulates patterning and morphogenesis of the pharyngeal arch-derived skeleton. *Dev Biol.* 2012; 369:65–75. [PubMed: 22709972]
- Szabo-Rogers HL, Geetha-Loganathan P, Whiting CJ, Nimmagadda S, Fu K, Richman JM. Novel skeletogenic patterning roles for the olfactory pit. *Development.* 2009; 136:219–29. [PubMed: 19056832]
- Szabo-Rogers HL, Smithers LE, Yakob W, Liu KJ. New directions in craniofacial morphogenesis. *Dev Biol.* 2010; 341:84–94. [PubMed: 19941846]

- Takada N, Appel B. swap70 Promotes neural precursor cell cycle exit and oligodendrocyte formation. *Molecular and Cellular Neuroscience*. 2011; 48:225–235. [PubMed: 21875669]
- Theveneau E, Mayor R. Neural crest delamination and migration: From epithelium-to-mesenchyme transition to collective cell migration. *Dev Biol*. 2012; 366:34–54. [PubMed: 22261150]
- Thisse C, Thisse B, Postlethwait JH. Expression of *snail2*, a second member of the zebrafish *snail* family, in cephalic mesendoderm and presumptive neural crest of wild-type and spadetail mutant embryos. *Dev Biol*. 1995; 172:86–99. [PubMed: 7589816]
- Thisse, B.; Pflumio, S.; Fürthauer, M.; Loppin, B.; Heyer, V.; Degraeve, A.; Woehl, R.; Lux, A.; Steffan, T.; Charbonnier, XQ.; Thisse, C. Expression of the zebrafish genome during embryogenesis (NIH R01 RR15402). ZFIN Direct Data Submission. 2001. (<http://zfin.org>)
- Toyama R, Gomez DM, Mana MD, Dawid IB. Sequence relationships and expression patterns of zebrafish *zic2* and *zic5* genes. *Gene Expr Patterns*. 2004; 4:345–50. [PubMed: 15053986]
- Tu CT, Yang TC, Huang HY, Tsai HJ. Zebrafish *arl6ip1* is required for neural crest development during embryogenesis. *PLoS One*. 2012; 7:e32899. [PubMed: 22427906]
- Vandepoele K, De Vos W, Taylor JS, Meyer A, Van de Peer Y. Major events in the genome evolution of vertebrates: paranome age and size differ considerably between ray-finned fishes and land vertebrates. *Proc Natl Acad Sci U S A*. 2004; 101:1638–43. [PubMed: 14757817]
- Vanderlaan G, Tyurina OV, Karlstrom RO, Chandrasekhar A. Gli function is essential for motor neuron induction in zebrafish. *Dev Biol*. 2005; 282:550–70. [PubMed: 15890329]
- Wada N, Javidan Y, Nelson S, Carney TJ, Kelsh RN, Schilling TF. Hedgehog signaling is required for cranial neural crest morphogenesis and chondrogenesis at the midline in the zebrafish skull. *Development*. 2005; 132:3977–88. [PubMed: 16049113]
- Warr N, Powles-Glover N, Chappell A, Robson J, Norris D, Arkell RM. *Zic2*-associated holoprosencephaly is caused by a transient defect in the organizer region during gastrulation. *Hum Mol Genet*. 2008; 17:2986–96. [PubMed: 18617531]
- Westerfield, M. A guide for the laboratory use of zebrafish (*Danio rerio*). 4. Univ. of Oregon Press; Eugene: 2000. The zebrafish book.
- Wilkie AO, Morriss-Kay GM. Genetics of craniofacial development and malformation. *Nat Rev Genet*. 2001; 2:458–68. [PubMed: 11389462]
- Yan YL, Hatta K, Riggleman B, Postlethwait JH. Expression of a type II collagen gene in the zebrafish embryonic axis. *Dev Dyn*. 1995; 203:363–76. [PubMed: 8589433]
- Yan YL, Willoughby J, Liu D, Crump JG, Wilson C, Miller CT, Singer A, Kimmel C, Westerfield M, Postlethwait JH. A pair of Sox: distinct and overlapping functions of zebrafish *sox9* co-orthologs in craniofacial and pectoral fin development. *Development*. 2005; 132:1069–83. [PubMed: 15689370]

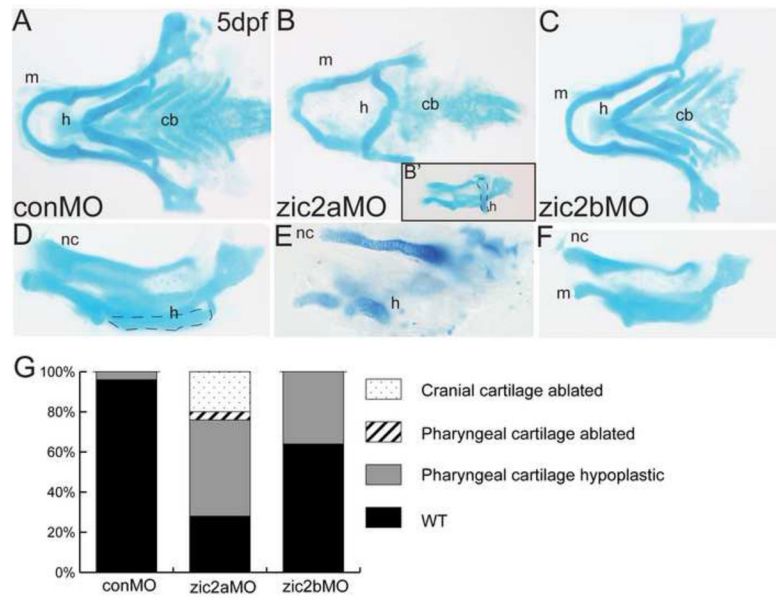


**Fig. 1. Zic2 is required for craniofacial development**

Alcian blue-stained cartilage in *zic2* morphants at 5 dpf. (A,D) Control morphants have wild-type pharyngeal and neurocranial cartilages (53/55, 6 exp.). (B) *Zic2a* morphants have variable craniofacial defects, including hypoplastic pharyngeal cartilages and an incorrectly angled hyoid arch (16/54, 5 exp.; outline in 1B'). (E) Severely affected *zic2a* morphants have more dramatic hypoplasia (10/54, 5 exp.) or ablation of anterior cartilages (11/54, not shown). (C,F) *Zic2b* morphants are either wild-type (45/70, 6 exp.) or develop shortened mandibular and hyoid arches (25/70, 6 exp.). (G) Penetrance of craniofacial defects in control and morphant embryos. A–C are dorsal views with anterior to the left. D–F are lateral views. Abbreviations: cb – ceratobranchials, h – hyoid, m – mandibular, nc – neurocranium.

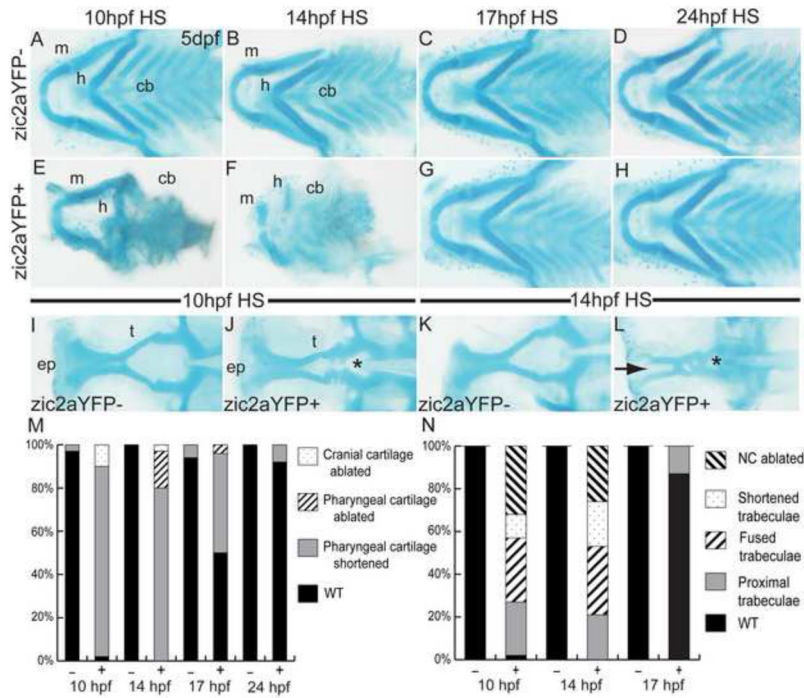


**Fig. 2. Craniofacial development is sensitive to early elevation of Zic2a levels**

Alcian blue-stained cartilage in heat-shocked *Tg(hsp70l:Gal4VP16);Tg(11XUAS:zic2aYFP)* embryos at 5dpf. (A,E) Heat shock (HS)-induced misexpression of Zic2aYFP at 10hpf has a variable effect on craniofacial cartilage, ranging from shortened mandibular and hyoid arches (45/51, 5 exp., shown in 2E) to absence of all anterior cartilages (5/51, 5 exp.). (B,F) Zic2aYFP induction at 14hpf has a similar effect, causing hypoplastic pharyngeal cartilages (29/36, 3 exp., shown in 2F) or ablation (7/36, 3 exp.). (C,G) Zic2aYFP induction at 17hpf causes less penetrant pharyngeal cartilage hypoplasia in overexpressors (12/24, 2 exp.). (D,H) Zic2aYFP induction at 24hpf has no effect on craniofacial cartilage (57/62, 4 exp.). (I,J) 10hpf HS causes a narrowing of the space between trabecular cartilages (13/53, 4 exp., asterisk in 2J) or complete fusion (16/53, 4 exp.). (K,L) Zic2aYFP induction at 14hpf causes fusion of the trabeculae (asterisk in 2L) and absence of the ethmoid plate (10/19, 1 exp., arrow in 2L), or ablation of the entire anterior neurocranium (5/19, 1 exp.). (M,N) Penetrance of cartilage defects following Zic2aYFP induction at specified timepoints. A–H are dissected pharyngeal cartilages, dorsal views, anterior to the left. I–L are dissected neurocranial cartilages, dorsal views, anterior to the left. Abbreviations: cb – ceratobranchials, ep – ethmoid plate, h – hyoid arch, m – mandibular arch, t – trabecular cartilages.

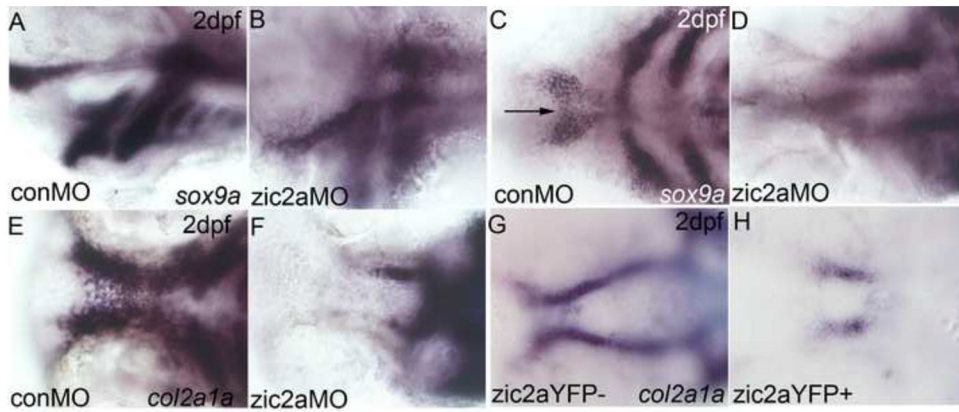


**Fig. 3. Zic2a regulates patterning of anterior chondrogenic condensations**

2dpf *zic2a* morphants (A–F) and overexpressors (G,H) stained by ISH for *col2a1a* or *sox9a*. (A,B) *Sox9a* expression is reduced in the posterior PAs of *Zic2a*-depleted embryos (18/20, 1 exp.). (C,D) *Zic2a* morphants have shortened trabeculae (18/20, 1 exp.) and lack the medial ethmoid plate (12/20, 1 exp., arrow in 3C). (E,F) Expression of *col2a1a* reiterates the shortened trabeculae and lack of ethmoid plate in *Zic2a*-depleted embryos (43/43, 2 exp.). (G,H) *Col2a1a* expression in wild-type siblings shows the bilateral trabeculae and ethmoid plate (67/107, 2 exp.). (H) The ethmoid plate is ablated and trabeculae are shortened by *Zic2a*YFP misexpression induced at 10hpf (38/67, 2 exp). A,B are lateral views. C–H are ventral views, anterior to the left.

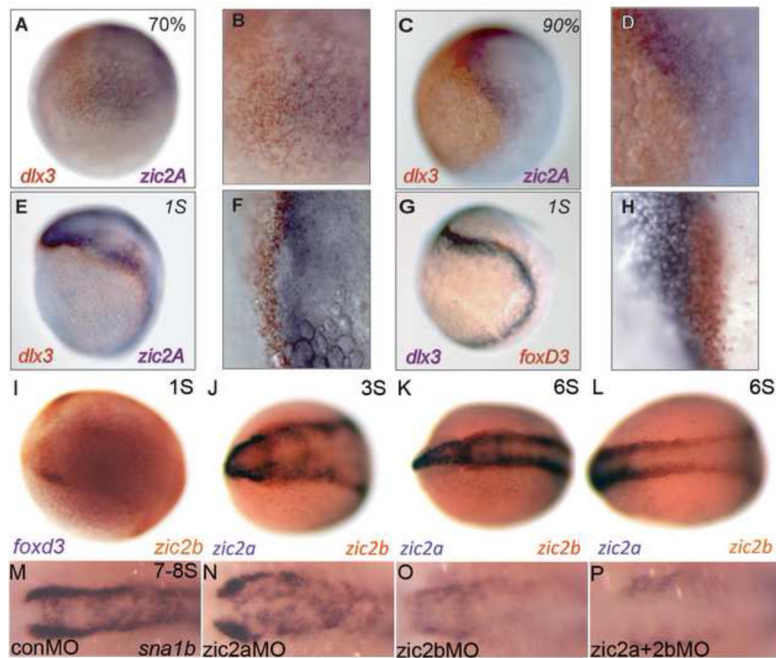


**Fig. 4. Zic2b promotes timely neural crest induction**

(A–L) Wild-type embryos stained by two-color ISH for expression of *dlx3b*, *foxd3*, *zic2a* and *zic2b*. (A,B) At 70% epiboly, weak expression of *dlx3b* (orange) and *zic2a* (purple) form two adjacent domains. (C,D) These domains are stronger by 90% epiboly but continue to overlap, suggesting the neural plate border is not completely formed. (E,F) At 1S, *dlx3b* (orange) and *zic2a* (purple) begin to separate. (G,H) *Foxd3* (orange) straddles the border beginning at 1S, overlapping neural and non-neural (*dlx3b*, purple) markers. (I) At 1S, NC marker *foxd3* (orange) and *zic2b* (purple) overlap at the neural plate border. (J,K) From 3–6S, *zic2b* (orange) is expressed in two anterior, bilateral domains from which *zic2a* (purple) is excluded. (L) *Zic2b* expression at the neural plate border extends into the posterior neural keel. (M,N) *Sna1b* expression is unchanged in *zic2a* morphants during early somitogenesis (37/48, 5 exp.). (O) *Zic2b* morphants have reduced (19/47, 5 exp.) or absent (16/47, 5 exp.) NC domains. (P) The *sna1b* domain is reduced (11/38, 5 exp.) or more frequently absent (24/38, 5 exp.) in double *zic2* morphants. A,C,E,G are lateral views, anterior to the right. B, D, F and H are high magnification images of A, C, E and G, respectively. I–P are dorsal views with anterior to the left.

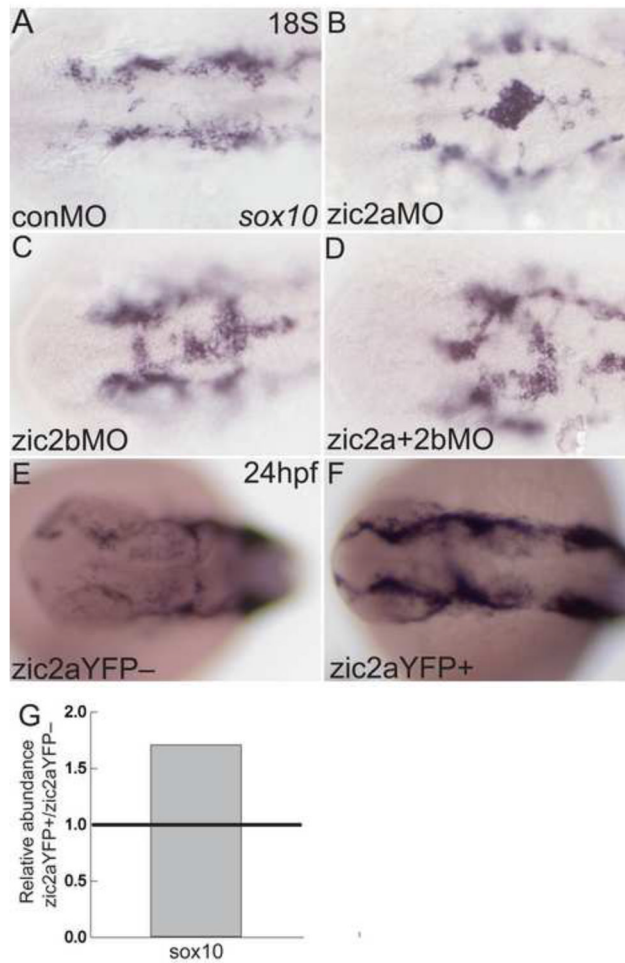


**Fig. 5. Zic2a and zic2b regulate neural crest migratory onset**

Morphant (A–D) or overexpressing embryos (E–F) stained by ISH for *sox10*. (A) At 18S, *sox10* is expressed in NC cells, which have exited the neural tube in control morphants (17/21, 3 experiments). (B,C) Single knockdown of Zic2a or Zic2b results in NC cells abnormally localized to the dorsal neural tube (8/12 *zic2a* morphants, 2 exp.; 14/32 *zic2b* morphants, 3 exp.). (D) Double Zic2 depletion causes a similar buildup of *sox10*-positive cells on the dorsal neural tube (7/10 embryos, 2 exp.). (E,F) Transgenic embryos were heat shocked at 10hpf to induce Zic2aYFP expression. Embryos expressing the *zic2a*YFP fusion protein have wild-type localization of NC cells, but increased *sox10* expression (20/30, 2 exp.). (G) Quantitative real-time PCR for *sox10* in 24hpf embryos after 10hpf HS. Relative abundance of *sox10* transcript averaged across two biological replicates. A–F are dorsal views, anterior to the left.

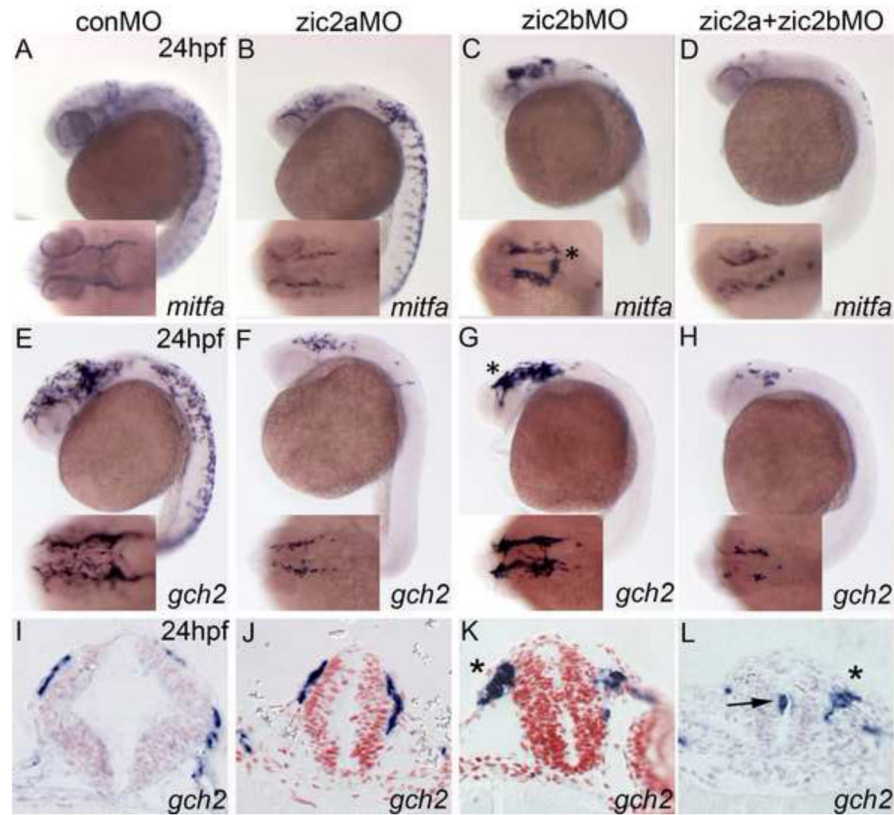


**Fig. 6. Zic2a and zic2b promote chromatophore development**

Zic2 morphant embryos stained by ISH for *mitfa* and *gch2* at 24hpf. (A,B) Zic2a knockdown causes a mild reduction of cranial melanophore progenitors, marked by *mitfa* expression (21/35, 3 exp.). (C) Zic2b knockdown dramatically reduces *mitfa* expression in the trunk (24/27, 3 exp.). (D) Knockdown of both Zic2 proteins reduces melanophores in both cranial and trunk regions (22/29, 3 exp.) and causes NC aggregation in the cranial region (12/24, 3 exp.). (E,F) Zic2a knockdown reduces xanthophore precursors, marked by *gch2* expression, in the cranial region (13/20, 3 exp.) and trunk region (16/22, 3 exp.). (G) Zic2b knockdown reduces trunk xanthophores (27/28, 3 exp.). (H) Double Zic2 knockdown decreases *gch2* at both cranial and trunk axial levels (17/20 affected, 3 exp.). (I,J) *Gch2*-expressing cells migrating on the midbrain are wild-type in *zic2a* morphants (3/3, 1 exp.). (K,L) Large aggregates of migrating NC cells are observed after Zic2b knockdown (1/3, 1 exp.; asterisks in C,G,K) and double Zic2 knockdown (2/3, 1 exp.; asterisk in 7L). A–H are lateral views with anterior to the left, with insets showing dorsal views of the same embryos. I–J are transverse sections through the midbrain.



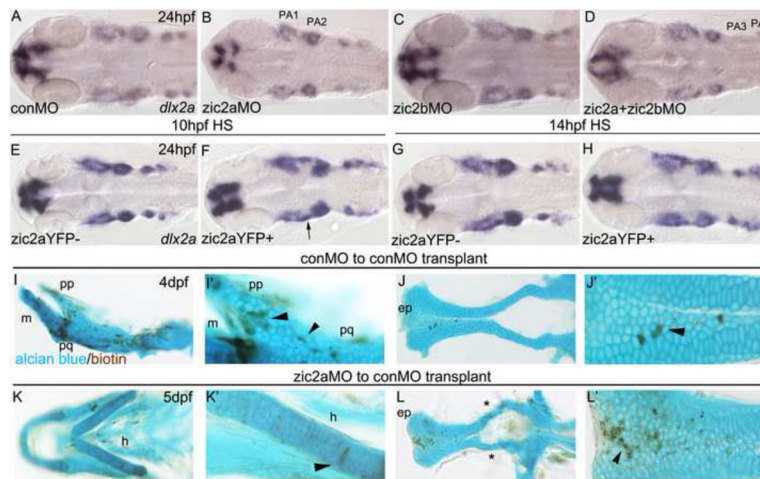


**Fig. 7. Pharyngeal arch primordia are mispatterned in response to changes in Zic2a levels**  
 (AH) Embryos stained by ISH for *dlx2a*. (A) Four streams of NC cells that populate the pharyngeal arches express *dlx2a* (42/44, 3 exp.). (B) The *dlx2a* domain is reduced in PA1 and 2 of *zic2a* morphants (13/30, 3 exp.). (C) *Zic2b* knockdown has no effect on *dlx2a* expression in the PAs (40/44, 3 exp.). (D) The first two pharyngeal arches are reduced in some double morphants (15/46, 3 exp.), while other embryos have a reduction of *dlx2a* in PA3 and PA4 (11/46, 3 exp., shown in D) or all four PAs (10/46, 3 exp.). (E,F) After HS induction at 10hpf, some *Zic2a*YFP-positive embryos are wild-type (13/64 embryos, 3 exp.), some have an elongated PA1 (21/64, see arrow in F) and some have reduced *dlx2a* staining in the arches (28/64). (G,H) *Dlx2a* expression remains unchanged after *Zic2a*YFP induction at 14hpf (15/17, 1 exp.). (I–L) Transplant host embryos stained for biotin and alcian blue at 4dpf. (I,J) Transplanted control morphant cells incorporated in the pterygoid process, palatoquadrate, and ethmoid plate of control morphant embryos (see arrowheads). (K,L) Transplanted *Zic2a*-deficient cells incorporated into the hyoid arch and the ethmoid plate of control morphant embryos. (L) Some control morphant host embryos develop with abnormal trabecular cartilages (see asterisks). A–H are dorsal views with anterior to the left. I–L are dissected pharyngeal and neurocranial cartilages. I', J', K' and L' are close-up views of I–L. Abbreviations: ep – ethmoid plate, h – hyoid, m - mandibular, pp – pterygoid process, pq – palatoquadrate.

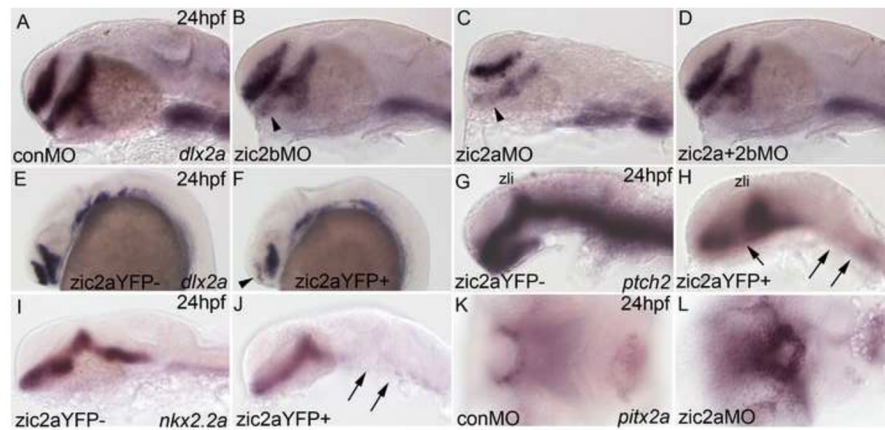


**Fig. 8. Zebrafish Zic2 patterns the ventral forebrain primordium**

Embryos stained by ISH for *dlx2a*, *nkx2.2a*, and *ptch2* at 24hpf and *pitx2a* at 3 dpf. (A) *Dlx2a* marks the telencephalon, prethalamus and hypothalamus in the developing forebrain of control morphants (42/44, 3 exp.). (B) *Zic2b* knockdown reduces *dlx2a* staining in the prethalamus (18/35, 3 exp., see arrowhead). (C) *Zic2a* knockdown reduces *dlx2a* in the prethalamus and hypothalamus, as previously described (see Sanek et al., 2008; 39/43, 3 exp.). (D) Double *zic* knockdown causes patterning defects similar to single *Zic2a* knockdown (46/46, 3 exp.). (E,F) *Zic2a*YFP induction at 10hpf strongly reduces *dlx2a* expression in the telencephalon (arrowhead in F) and hypothalamus (61/92, 4 exp.). (G,H) *Ptch2* expression is ablated in the hindbrain and spinal cord and reduced in the medial diencephalon of *Zic2a*YFP-expressing embryos, but maintained in the ZLI (49/57, 2 exp., see arrows in H). (I,J) *Zic2a*YFP induction between 10 and 11hpf ablates *nkx2.2a* expression in the hindbrain (35/35 embryos, 2 exp., arrows in J). (K,L) The stomodeum of *zic2a* morphants is decreased in size (55/56, 4 exp.). A–J are lateral views, K, L are ventral views, anterior to the left. Abbreviations: zli – zona limitans intrathalamica.